Colloidal Ordered Assemblies in a Polymer Shell – A Novel Type of Magnetic Nanobeads for Theranostic Applications

Nadja C. Bigall, [†, ‡], Claire Wilhelm[††], Marie-Lys Beoutis[††], Mar García-Hernandez[‡‡], Abid A. Khan[§], Cinzia Giannini[§§], Antoni Sánchez-Ferrer[▽], Raffaele Mezzenga[▽], Maria Elena Materia[‡], Miguel A. Garcia[▽▽], Florence Gazeau[††], Alexander M. Bittner[§], Liberato Manna[‡], Teresa Pellegrino[‡,¬] *

[‡] Istituto Italiano di Tecnologia,
Via Morego 30, I-16163 Genova (Italy)
[††] Univ Paris Diderot, CNRS, UMR7057
Lab MSC, F-75205 Paris 13 (France)
[‡‡] Instituto de Ciencia de Materiales de Madrid, CSIC
E-28049 Madrid (Spain)
[§] CIC NanoGUNE Consolider
Donostia San Sebastian E-20018 (Spain)
[§§] CNR, Ist. Crystallog,
I-70126 Bari (Italy)
[▽] ETH Zürich, Institute of Food, Nutrition & Health,
8092 Zürich (Switzerland).
[▽▽] Instituto de Cerámica y Consejo Vidrio, CSIC & IMDEA Nanociencia
E-28049, Madrid (Spain)
[¬] Nanoscience Institute of CNR, NNL,
Via Arnesano, I-73100 Lecce (Italy)

KEYWORDS *colloidal assemblies, polymer shell, MRI contrast agents, magnetic nanoparticles*

Determination of the necessary acetonitrile concentration to synthesize polymer-COAs

Solubility tests revealed that the formation of stable COAs with high order occurred in the absence of the polymer, and already at volume addition of acetonitrile at which the polymer was still sufficiently soluble. This was tested in the following way: first, the amount of acetonitrile which caused the COAs to form in absence of the polymer was identified. Second, the same amount of acetonitrile was added to a polymer-in-tetrahydrofurane solution in absence of the nanoparticles, which did not cause the solution to become turbid.

Additional information about COAs and polymer-COAs

In the following section, the results of more synthetic experiments and of additional characterizations for obtaining COAs and polymer-COAs are shown.

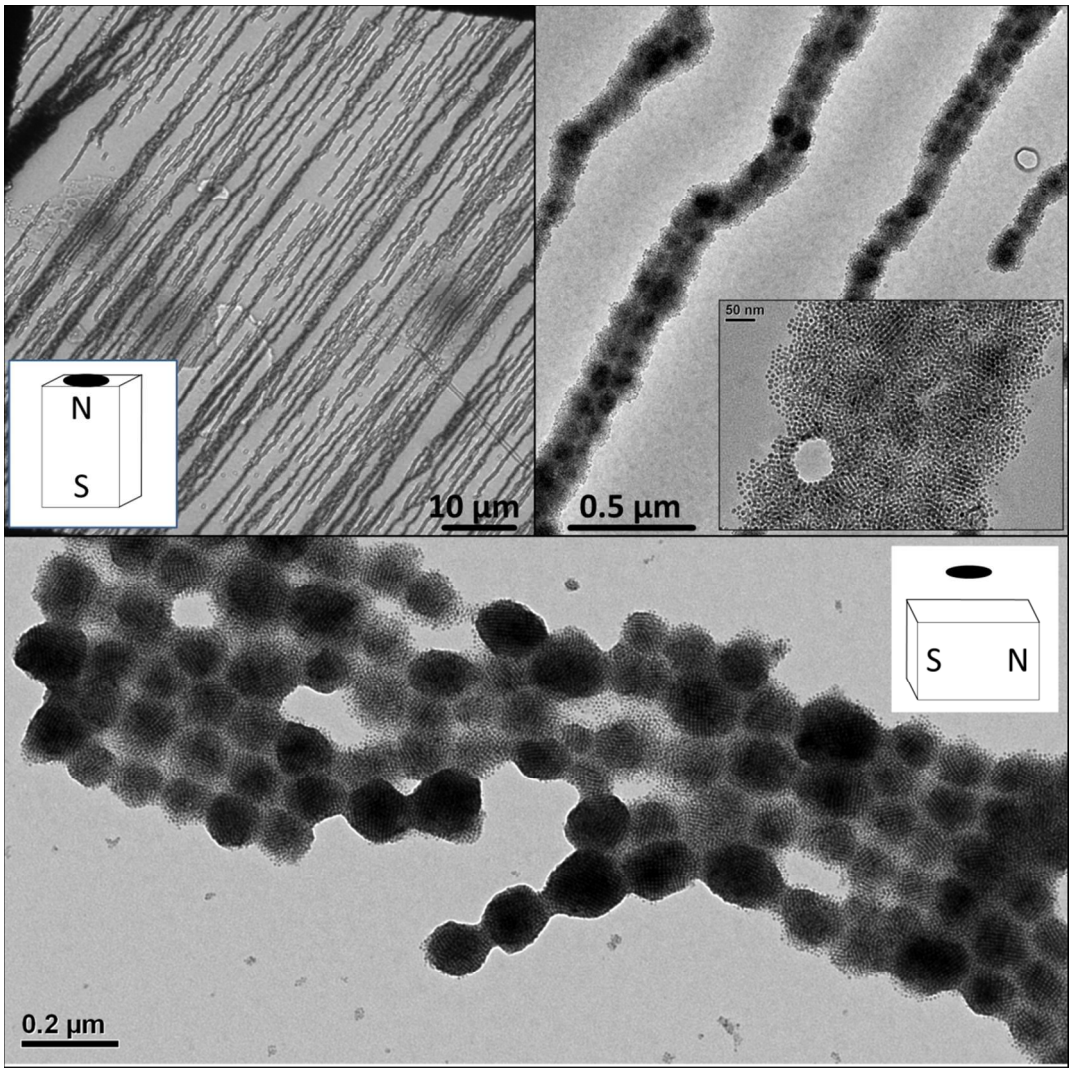

Figure SI1. *TEM images of COAs dried in the presence of a magnet. (top) Overview of a TEM grid mesh showing the large scale drying along the magnetic field lines (left), and higher magnification images (right and inset right) proving that the COAs partly retain their shape during the drying process. (bottom) higher magnification TEM image of a dried assembly of the COAs when dried at a different position with respect to the magnet (the white insets indicate the position of the TEM grid in respect to the magnet).*

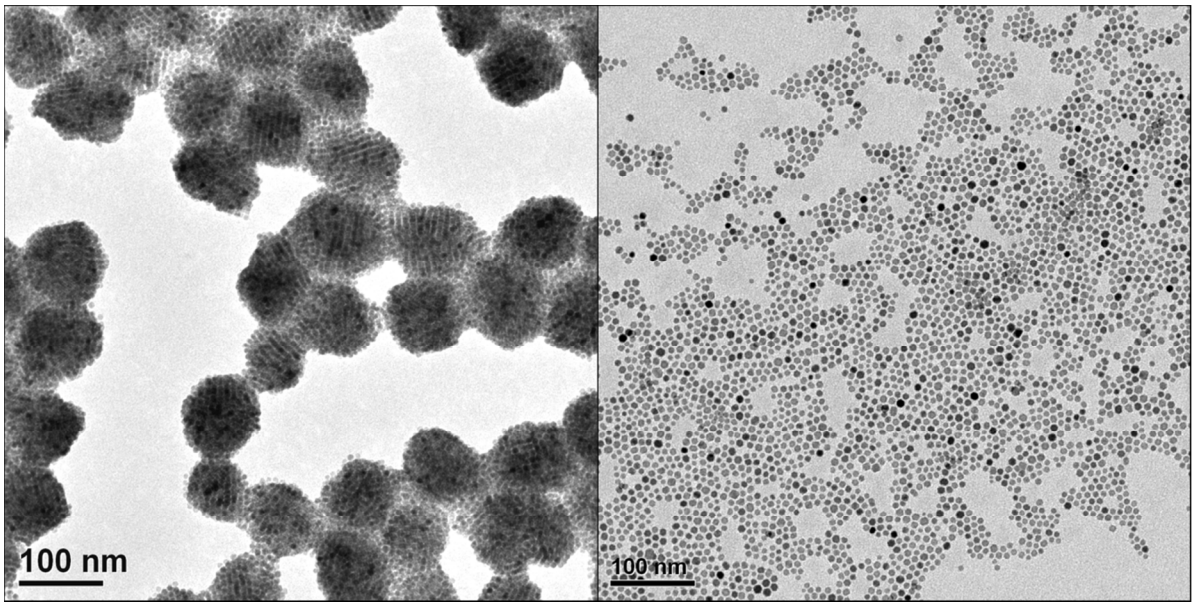

Figure SI2. *TEM images of COAs synthesized by dissolving 0.1 nmol $MnFe_2O_4$ nanoparticles in 200uL dry tetrahydrofurane. After shaking for 30 min, 0.8 mL ACN were added with a rate of 250 µL/min. COAs dried on a TEM grid (left). When drying the COAs and re-dissolving them in pure tetrahydrofurane, the assemblies were destroyed while the nanoparticles could be redispersed again (right) proving the reversibility of the assembly formation.*

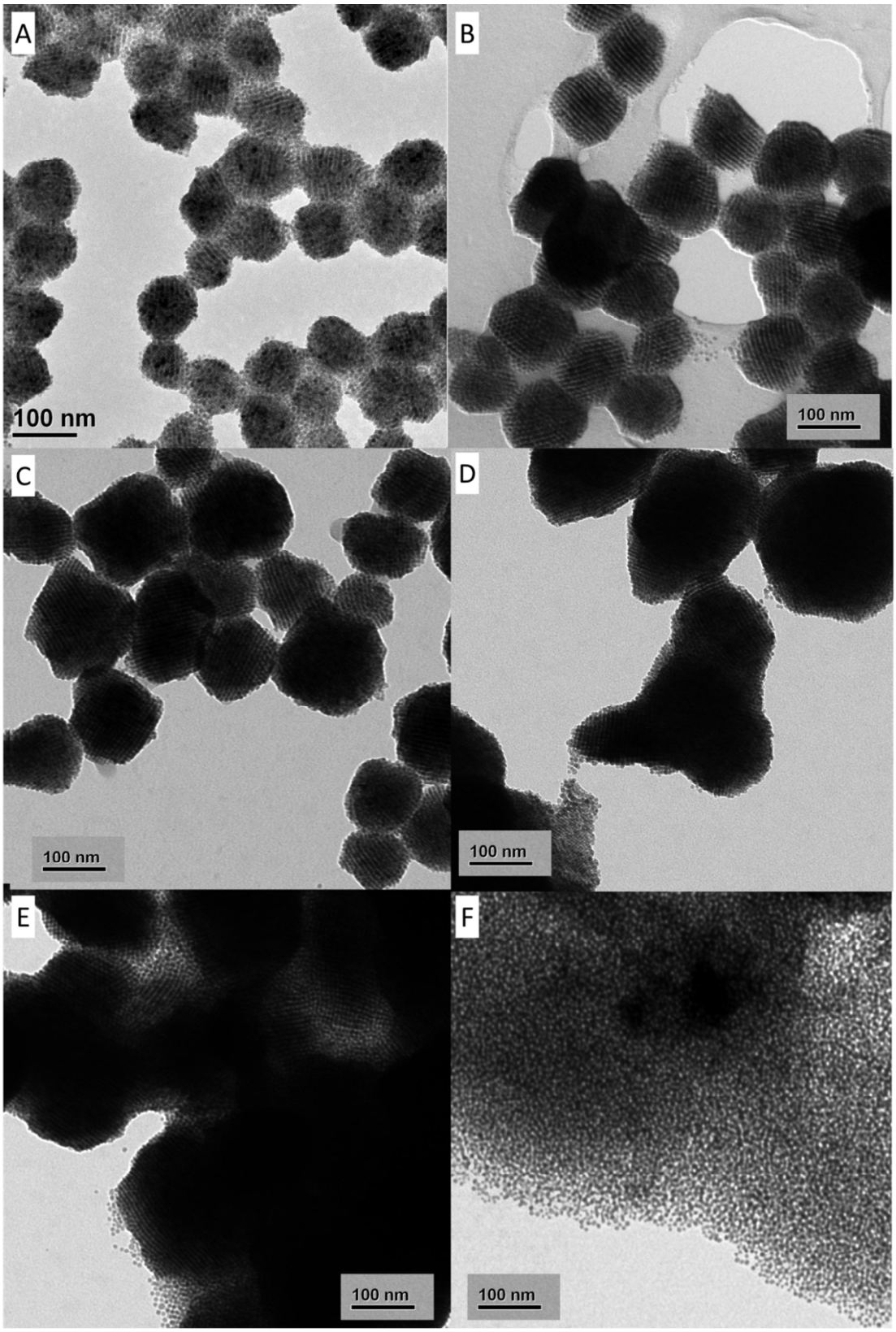

Figure SI3. *TEM images of COAs from various de-stabilization agents, namely (A) acetonitrile, (B) dimethyl sulfoxide, (C) dimethylformamide, (D) methanol, (E) ethanol, (F) water. The change*

in polarity of the solution upon addition of the solvent promotes hydrophobic interactions among surfactant-coated nanoparticles and hence the aggregation of the nanoparticles. The kinetics of the aggregation processes seem to be controlled by the solvent polarity added to the THF. While with water no ordering occurs, with all other investigated de-stabilizing agents ordering of the assembled nanoparticles was observed. The sizes of the observed superstructures increased from A to F. In general, in a more polar solvent like water, the nanoparticle aggregation occurs so quickly that the nanoparticles cannot rearrange with respect to each other. By reducing the polarity of the solvent, for example using ethanol or methanol, the nanoparticle aggregation is slower and therefore a better ordering can be observed. However, in ethanol and methanol, the aggregation tends to be too slow so that the agglomerates are getting too big, no solubility of the final aggregates is observed. The best results were achieved when using solvents in which the nanoparticles tend to precipitate quickly enough to form many aggregation seeds but slowly enough so that they aggregate in a concerted way; then, the resulting aggregates were soluble in the final mixture of solvents. In this case, the best control over the final nanostructures could be achieved.

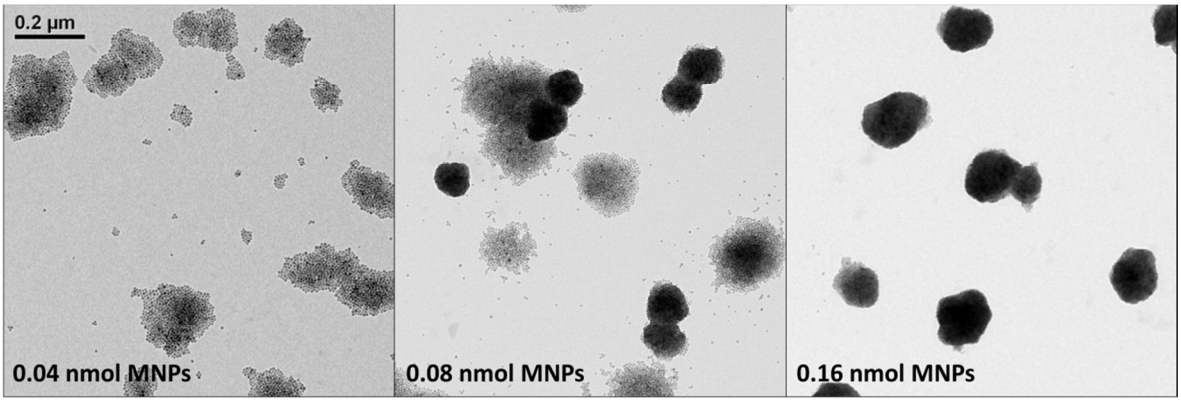

Figure SI4. *TEM images of COAs prepared by the addition of 0.1 mL acetonitrile to a solution of (left) 40 pm, (center) 80 pm and (right) 160 pm magnetic nanoparticles dispersed in 0.2 mL of tetrahydrofurane. In all three cases, the TEM grids were prepared 20 min after the addition of the acetonitrile. The scale bar corresponds for 0.2 µm and is the same for all images.*

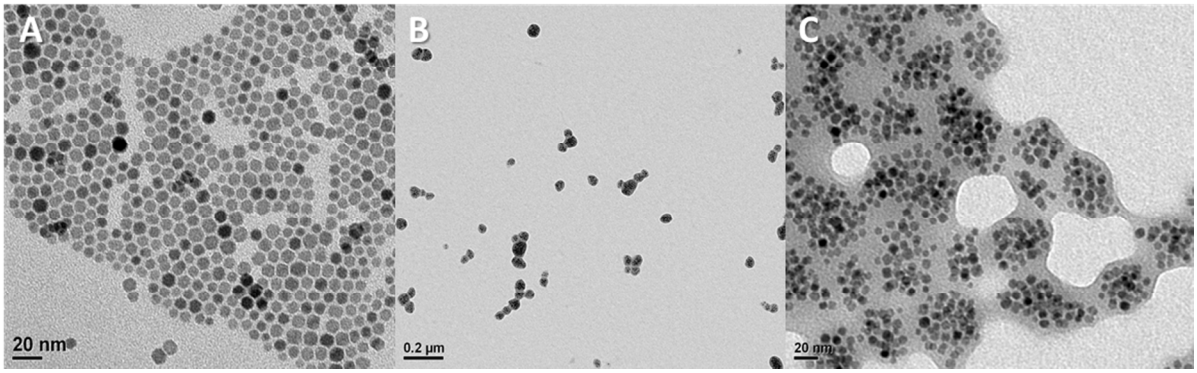

Figure SI 5. *TEM images of (A) the manganese iron oxide nanoparticles used for this work and (B,C) of the typical MNB sample as-prepared when using the same amount of polymer and nanoparticles as for the polymer-COAs.*

Fourier transform infrared (FT-IR) spectroscopy.

FTIR spectra were recorded with a Bruker vertex 70v Fourier transform infrared spectrometer equipped with an ATR cell. The sample preparation was conducted by drop-casting a small amount of the sample solution directly on the ATR cell followed by subsequent evaporation of the solvent under a nitrogen flux.

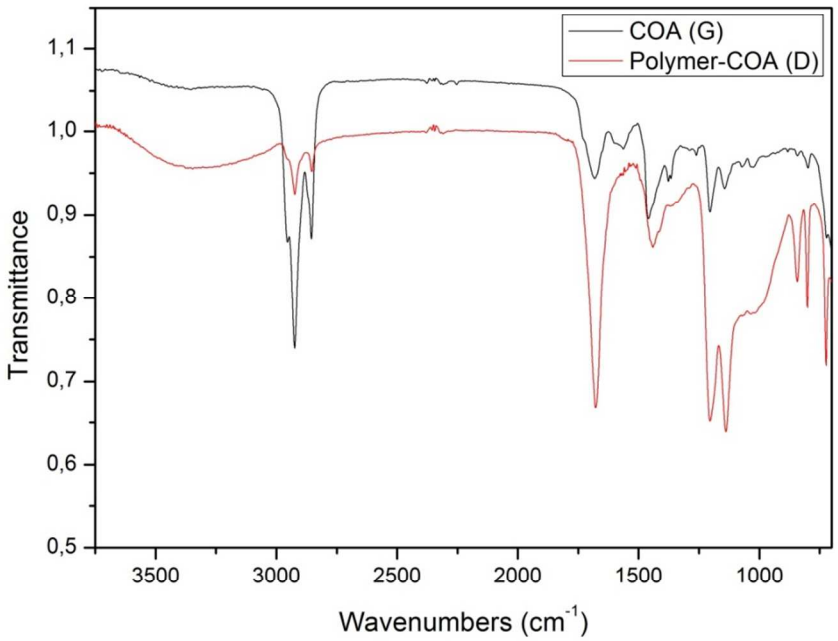

Figure SI6. *FTIR spectra of the samples COA (G) (black line) and Polymer-COA (D) (red line). In the COA (G) spectrum, the presence of surfactant molecules at the surface of the*

nanoclusters, deriving from that present at the nanoparticle surface (hexadecanediol, dodecylamine and lauric acid) are shown by two broad peaks at 2850 and 2920 cm^{-1} due to the methyl and methylene groups (stretching C-H). Besides, many others peaks can be ascribed to the surfactant molecules such as those at 1680 cm^{-1} and at 1200 and 1150 cm^{-1} due to the carboxylic groups (stretching C=O and stretching C-O), and the peaks between 1500 and 700 cm^{-1} due to the bending of different groups (C-O, C=O and C-H).

In the spectrum of the sample Polymer-COA (D) many of the peaks present also in the COA spectrum (stretching and bending of C-H, C=O, C-O) are visible. However, due to the presence of the polymer poly(maleic anhydride-*alt*-1-octadecene) at the surface of the COAs (sample D), the peaks related to the carboxylic groups are much more intense (1680 cm^{-1} stretching C=O, 1200 and 1150 cm^{-1} stretching C-O). Moreover, in the spectrum of polymer-COA (sample D), also a broad peak around 3320 cm^{-1} can be observed, which is attributed to the carboxylic acid group (stretching O-H) and therefore confirms the presence of open anhydride groups on the surface of the polymer-COAs. Furthermore, the decrease of intensity for the two peaks at 2850 and 2920 cm^{-1} (attributed to C-H stretching of the methyl and methylene groups), is possibly due to the intercalation of the polymer octadecene chains with the surfactant chains of the nanoparticles.

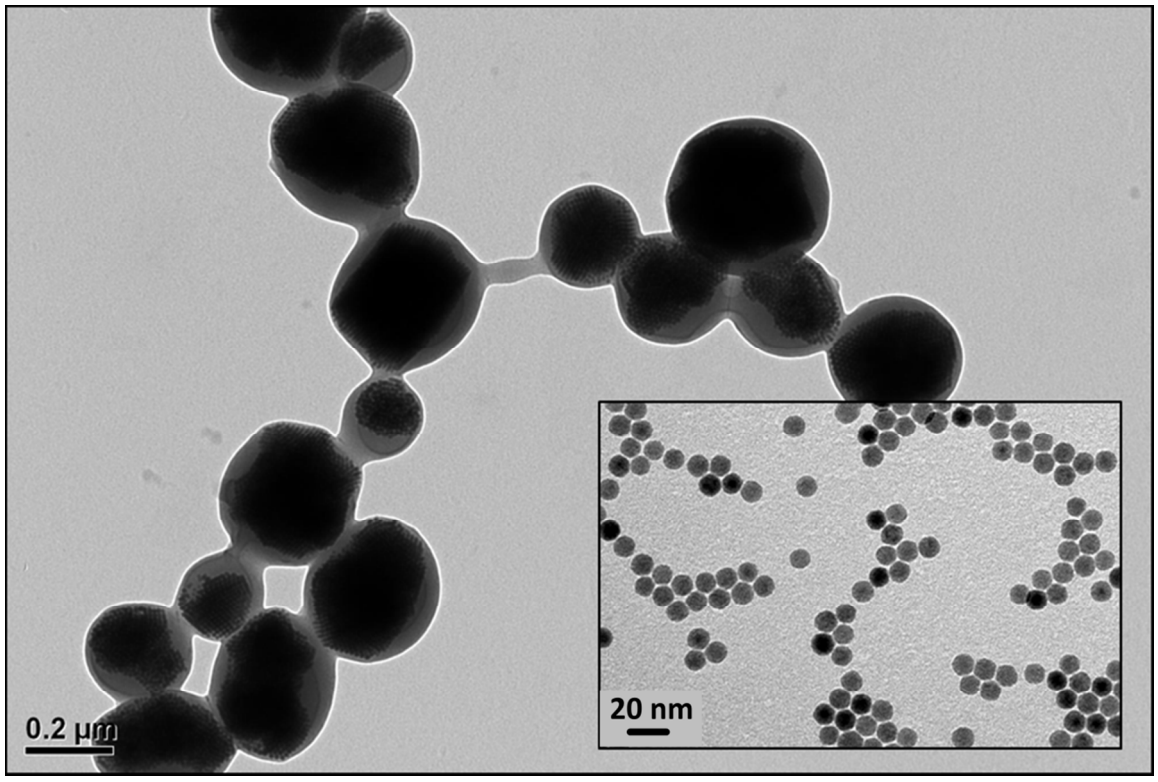

Figure SI7. *TEM images of polymer-COAs prepared from a different type of magnetic nanoparticles (synthesized with an oleic acid to iron oxide hydroxide ratio of 4:1 following the method of ref.*[12] *with an average diameter of 9.2 nm see inset) For the polymer-COA synthesis 5 µL of the nanoparticles were dried and re-dissolved in 195 µL tetrahydrofurane. After shaking for 15 min at 1000 rpm, 0.2 mL ACN were dropped with a rate of 0.1 mL/min. 7 min after the addition of the ACN, 15 µL PC18 were added. 30 min later, 1.4 mL ACN were added with a rate of 0.125 mL/min. In this case, the dispersion of the colloidal ordered assemblies was only stable in the time range of several minutes, while the dispersion of the CAPS was stable for several days.*

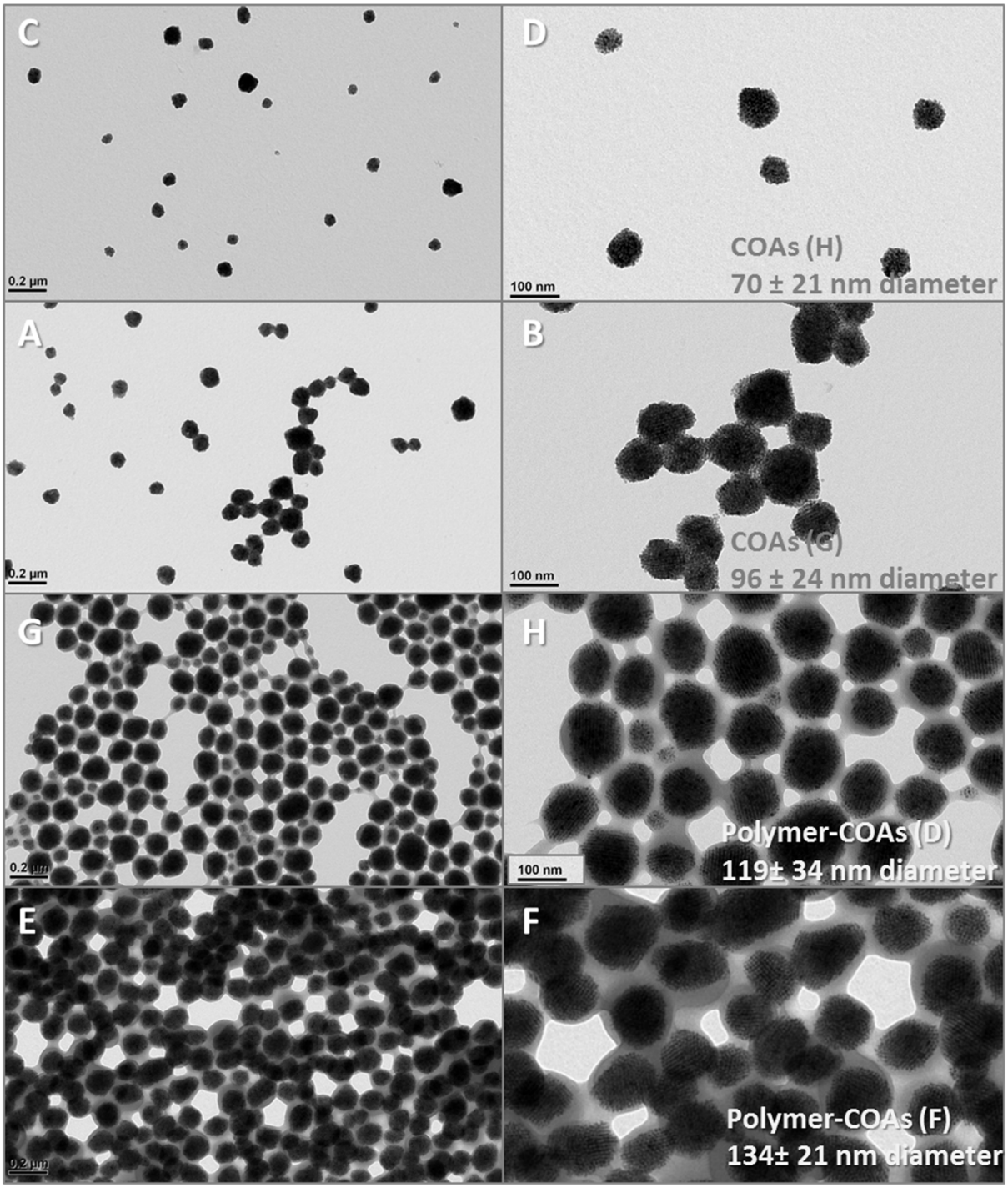

Figure SI8. *TEM images in two different magnifications (left and right, respectively) of the different samples compared in this study.(A,B) COAs of 70 nm diameter (sample H), (C,D) COAs of 96 nm diameter (sample G), (E, F) polymer-COAs of 119 nm diameter (sample D), and (G, H) polmer-COAs of 134 nm diameter (sample F).*

Dynamic Light Scattering (DLS) Characterization

Dynamic light measurements were performed on a Zetasizer Nano ZS90 (Malvern, USA) equipped with a 4.0 mW He-Ne laser operating at 633 nm and an avalanche photodiode detector. The hydrodynamic diameter was measured by DLS of a solution of colloidal ordered assemblies in ACN/THF (9:1) mixture for the samples COA (H) and COA (G), and of a solution of polymer embedded colloidal ordered assemblies in milliQ water for the samples Polymer-COA (D) and Polymer-COA (F). The measurements were conducted with a glass cuvette for the samples COA (H) and COA (G), setting 1.350 as the dispersant refractive index and 0.3800 cP as the viscosity. For the samples Polymer-COA (D) and Polymer-COA (F), instead, a cell type ZEN0112-low volume disposable sizing cuvette was used, setting 1.330 as the refractive index and 0.8869 cP as the viscosity. The measurements were performed with 173° backscatter (NIBS default) as angle of detection, the measurement duration was set automatic and three was the number of measurements.

The zeta potential for the samples Polymer-COA (D) and Polymer-COA (F) was also measured by DLS on a solution of polymer embedded colloidal ordered assemblies in milliQ water. The measurements were done on a clear disposable zeta cell, setting 1.330 as the dispersant refractive index and 0.8877 cP as the viscosity.

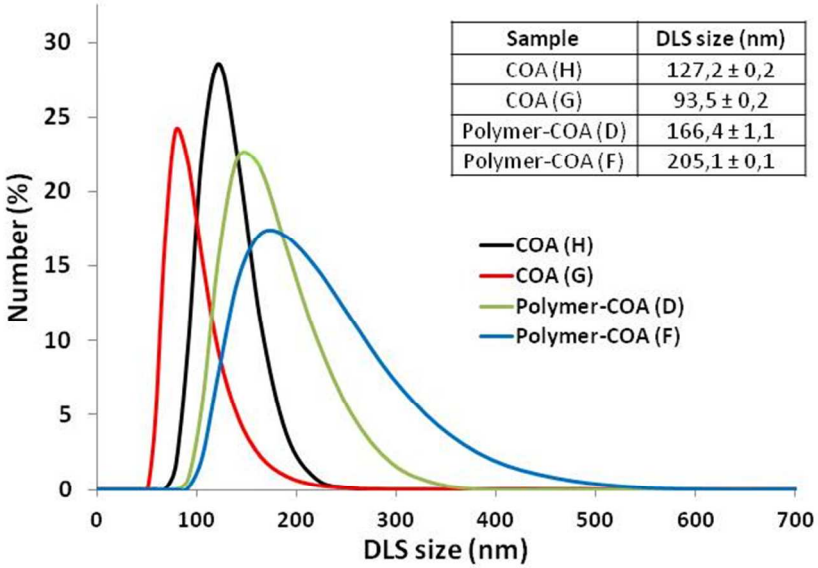

Figure SI9. *Comparison of the hydrodynamic diameters measured by DLS for the colloidal ordered assemblies. The size of the colloidal assemblies increases when they are enwrapped by the polymer (sample H corresponds to sample D and sample G corresponds to sample F). For the polymer-COA in water we observed negative zeta potentials of -45 mV and -33.5 mV for the samples polymer-COA (D) and polymer-COA(F), which is likely due to the presence of carboxyl groups at the surface of the polymer beads.*

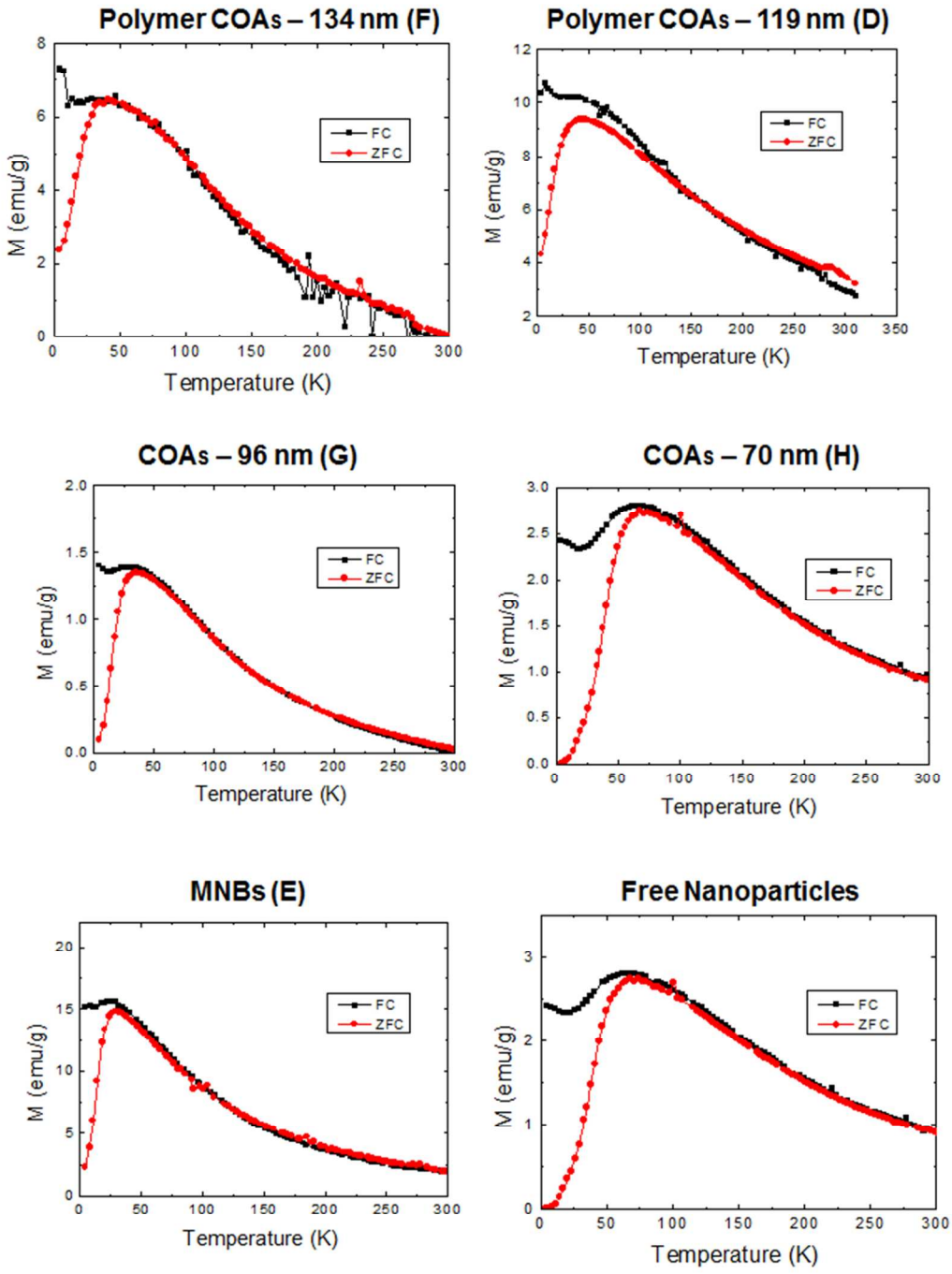

Figure SI10. *Thermal dependence of the magnetization upon field cooling (FC) and zero field cooling (ZFC) protocols. The cooling applied field was* H_{FC}*=5 T while the field applied during the measurement was Happ=50 Oe. The blocking temperature (TB, the maximum of the FCZ curve) and the irreversibility temperature (TIRR, temperature for which both, FC and ZFC*

curves, collapse) are almost identical. These results points out that that magnetic disorder, due to inter-particle interactions, is very weak.

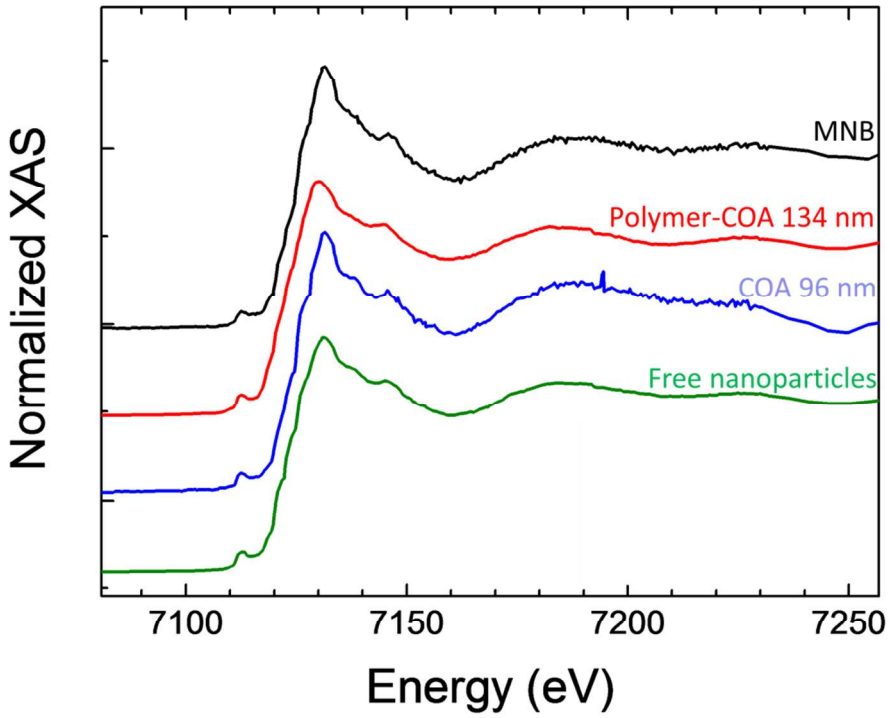

Figure SI11. *XAS spectra of the samples measured at the Fe K-edge (7112 eV) of the samples. Within the experimental resolution we did not observe variation in the edge position (related to the Fe oxidation state) that corresponds to* Fe^{+3}*. Neither the profile of the curves above the edge show significant differences in the electronic structure of the individual nanoparticles.*

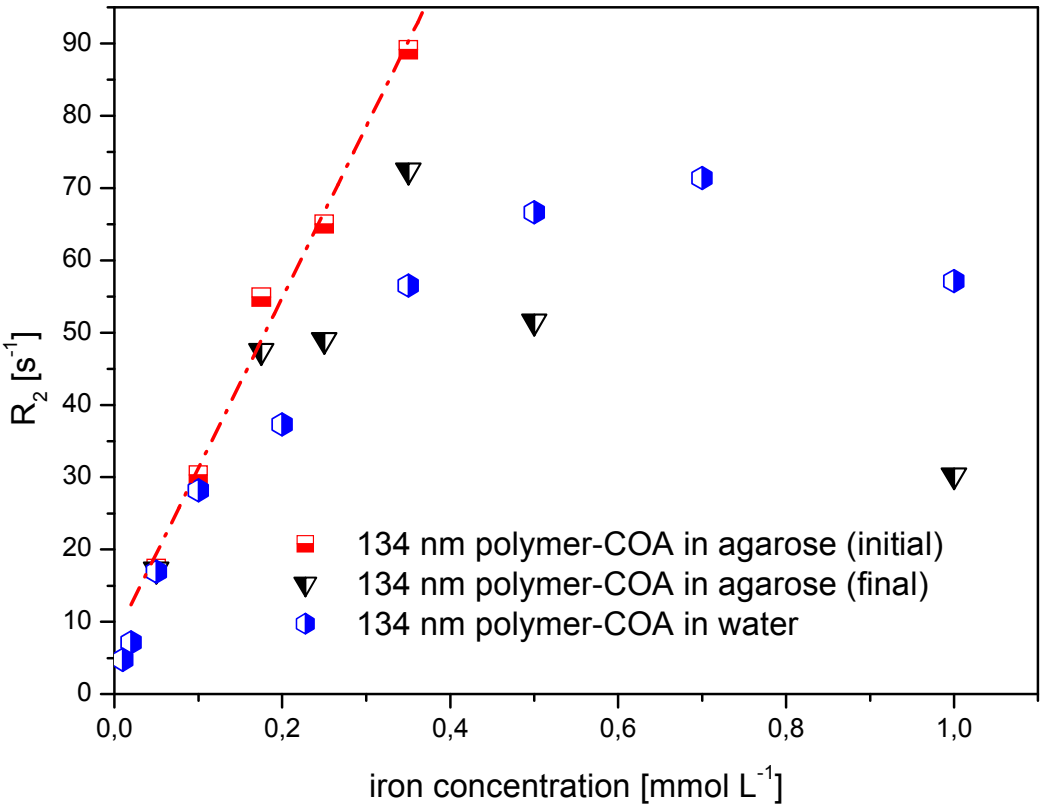

Figure SI12. *Relaxation times of 134 nm CAPS in agarose gel as a function of the CAPS concentrations measured in (blue) pure water, and in (red) a 0.3 % agarose gel. However, even in the agarose gel, after a long-term measurement (black), no linear concentration behavior was observed, especially for higher concentrations, indicating that also here field-induced agglomeration took place.*